Nano Bi_2O_3-TiO_2: An efficient and reusable catalyst for the synthesis of hydrazone derivatives

M. Jebastin Sonia Jas[1,3] G. Marimuthu[2*] And B. Prithivirajan[1]
[1]Research and development centre, Bharathiaruniversity, Coimbatore, 641046 India.
Email: gmarimuuthu@gmail.com
[2]Department of Chemistry, Swami Dayananda College of Arts and Science, Manjakkudi,Tiruvarur District-612610
[3] Department of Chemistry ,IFET College of Engineering, Villupuram

Abstract

Nano Bi_2O_3 supported on TiO_2 (Nano Bi_2O_3-TiO_2) as a solid was found to be an effective and reusable catalyst for the condensation reaction of chalcone and substituted hydrazides to afford the hydrazone derivatives (4a-e) at 100^0C under ethanol solvent conditions. The efficacy of the catalyst was examined in the reaction of 3-((E)-3-(2-amino-3,5-dibromophenyl)acryloyl)benzonitrile with benzohydrazide. The catalyst has been recovered and its reusability confirmed in 5 runs. A plausible mechanism of condensation has also been suggested.

Keywords : Nanocatalyst, chalcone, hydrazone, catalytic efficiency.

1.1.Introduction

Hydrazones containing an azometine -NHN=CH proton are synthesized by heating the appropriate substituted hydrazines/hydrazides with aldehydes and ketones like chalcone in solvents like ethanol, methanol, tetrahydrofuran, butanol, glacial acetic acid, ethanolglacial acetic acid [1]. Another synthetic route for the synthesis of hydrazones is the coupling of aryldiazonium salts with active hydrogen compounds. Many effective compounds, such as iproniazide and isocarboxazide, are synthesized by reduction of hydrazide-hydrazones. Iproniazide, like INH, is used in the treatment of tuberculosis. It has also displays an antidepressant effect and patients appear to have a better mood during the treatment. Another clinically effective hydrazide-hydrazones is nifuroxazide, which is used as an intestinal antiseptic. As a classical approach for the synthesis of hydrazone derivatives, condensation of carbonyl compounds and hydrazides is the most widely employed strategy, but it requires harsh dehydrating conditions.[2] Some acid catalysts such as glacial acetic acid,[3] SiO_2/H_2SO_4,[4] polystyrene sulfonic acid,[5] $Mg(ClO_4)_2$,[6] zeolites,[7] Dowex (strongly acidic cationic exchange resin) polymer,[8] choline chloride–oxalic acid,[9] and $[Et_3NH]$ $[HSO_4]$[10] have been developed to promote this reaction. This reaction has also been performed under ultrasonic irradiation[11] or microwave irradiation,[12] or by the kneading ball-milling technique.[13]

Although these protocols were efficient in many cases for synthesis of hydrazone derivatives, sometimes some methods suffer from one or more disadvantages such as the use of volatile organic solvents, unsatisfactory yields, over oxidization of aldehydes to the carboxylic acids, long reaction times, high temperature, difficulties in the product isolation, the lack of generality, or the requirement for special apparatus. In particular, many protecting groups are deprotected easily under acidic conditions. Thus, the development of a more efficient method for synthesis of hydrazone derivatives under environmentally benign conditions is still highly desirable. The nanocatalysts are highly selective, reactive, and stable; thereby it supersedes the conventional catalyst. Nanoparticles with a diameter of less than 10 nm have generated intense interest over the past decade due to their high potential applications in areas such as sensors, nanoscale electronics, catalysis, and optics. The catalytic activity of nanoparticles is affected by size; therefore, the relative ratio of surface atom types changes dramatically with varying particle size. Nanocatalyst is not only used in organic transformation but also it has various applications [14-15]. These nanocatalysts can be prepared by various methods [16-19]. The size and nature of nanocatalyst varies on the type of method used for preparation [20-27]. Based on the requirement, the method of preparation can be selected. Herein, we descried the use of BiO_3/TiO_2 as a catalyst to promote the condensation of hydrazides with chalcone compounds for synthesis of hydrazones (Scheme 2)

1.2 Experimental

The syntheses of Bi_2O_3-TiO_2 nanocomposite material Bismuth nitrate penta hydrate, Nitric acid and NH_4OH,Rhodamine 6G (Rh 6G) dyeandethanol solution were reagent of Sigma Aldrich on company and used as suchotherwise washed were prepared by using deionized water.

1.2.1. Preparation of Bi_2O_3-TiO_2nonocomposite material by precipitation method

The Bi_2O_3-TiO_2nanocomposite material was synthesized by precipitation method. Initially Bismuth nitrate penta hydrate were dissolved in anhydrous ethanol solution A and tetra isopropylortho titanate were in ethanol is taken as another solution B the solution Ais added to Solution beaker B and stirred well. To this pH of the solution was adjusted to about 9 by the addition of nitric acid solution 5 mL was added and NH_4OH is added at room temperature under vigorous stirring until the precipitate formed. The obtained precipitate was filtered and washed with water and ethanol. Then the precipitate was collected and dried on oven at 100^oC for 12 hrs. The resulting powder was finally calcinated at 450^oC at 4 hrs.

1.2.2. Characterization

Ultraviolet and visible (UV-VIS) absorbance spectra were measured over a range of 800-200 nm with a Shimadzu UV-1650PC recording spectrometer using a quartz cell with 10 mm of optical path length. High resolution Scanning Electron Microscopy (HR-SEM) as well as Elementary Dispersive X-ray (EDX) evaluation experiments were performed on a FEI Quanta FEG 200 instrument with EDX analyzer facility at 25^0C. The nanoparticles size and structure

verifications were done by Transmission Electron Microscopy (HR-TEM) making use of PHILIPS CM200. Each spectrum was recorded with an acquisition time of 18s. XRD spectrum was recorded on the X'PERT PRO model X-ray diffractometer from Pan Analytical instruments operated at a voltage of 40 kV and also a current of 30 mA with Cu Ka radiation. Photoluminescence (PL) spectra at a room temperature were recorded using a Perkin-Elmer LS 55 fluorescence spectrometer.

1.3.HR -SEM with EDX analysis

The HR-SEM image of Bi_2O_3-TiO_2nanocomposite material while it is shown in **Fig.1a** image of particle is in from of aggregates and uniformly distributed in various sized and nanospherical chain structure **Fig.1. (b)** EDX analysis confirm that only Ti, Bi and O are present in Bi_2O_3-TiO_2nanocomposite material.

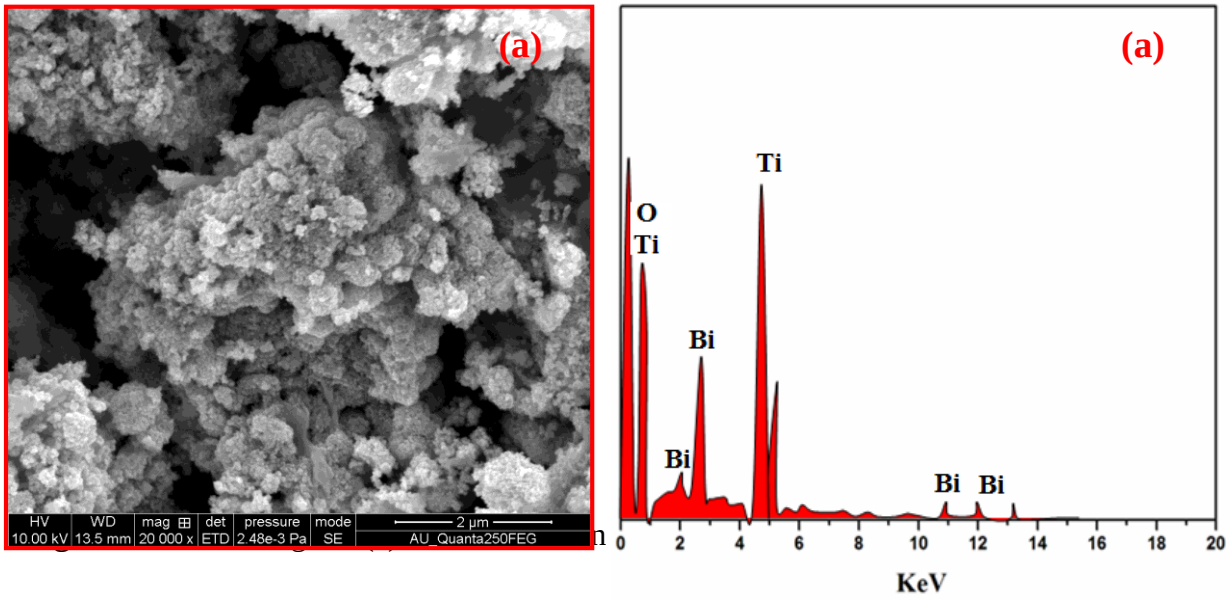

1.4.HR-TEM analysis

The High-resolution transmission electron microscope measurements of Bi_2O_3-TiO_2nanocomposite material are shown in **Fig 2a** it is established that the presence of particles are depicted from the HR-TEM micrographs of the mixed nanoparticles at 100 nm as nano spherical shaped structure. **Fig 2b** The represented an image profile and **Fig 2c** particle size distribution 0.281 nm by selected particle area highlighted show in **Fig 2a**.

1.5.XRDanalysis

The XRD spectra of TiO_2 and Bi_2O_3-TiO_2nanocomposite material are shown in **Fig 3** respectively. According to the crystal structure spectra, the well defined peaks typical of TiO_2 are clearly noticed. This is in compliance with the reports of the norms of the Joint Committee on Powder Diffraction Standard JCPDS card no. 21-1272. Samples give six distinctive TiO_2 peak in

the Figure 4a at 25, 29.91, 38.0, 47.87, 56.92, 64.5 and 74.74 are the diffractions of the TiO_2 (1 0 1), (0 0 4), (2 0 0), (1 0 5) and (2 0 4) crystal planes (anatase TiO_2)

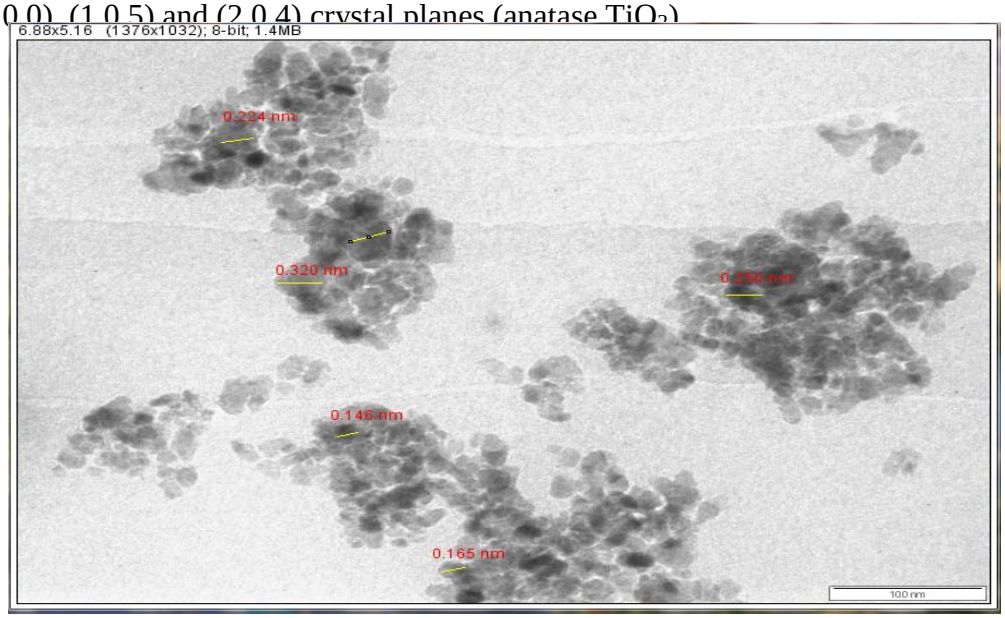

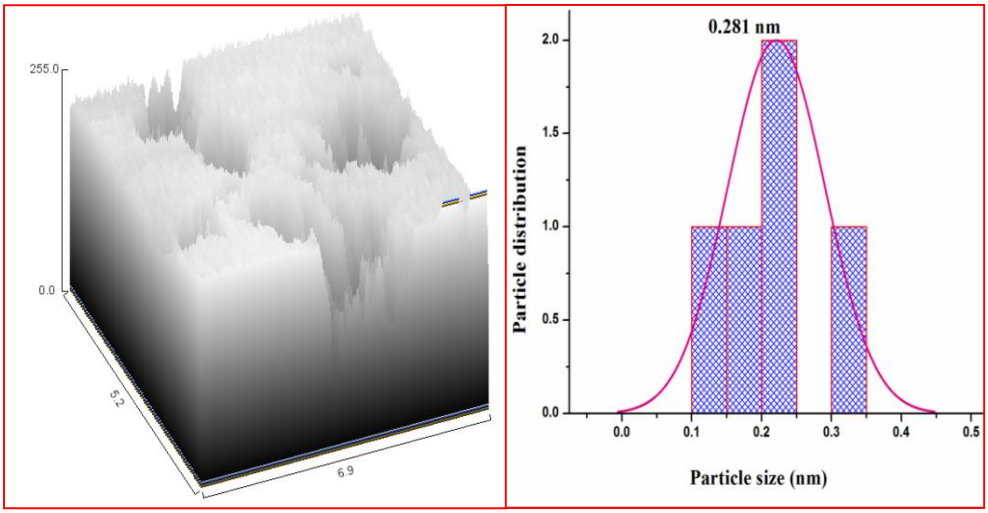

Fig.2. HR-TEM analysis of Bi_2O_3-TiO_2 nanocomposite material (a) TEM Image (b) Surface plot and (c) particle size in selected area highlighted fig (a)

The XRD spectrum of peaks observed at 30.10, 33.5 and 46.3^0 it shown in **Fig 3** correspond to (012), (-122), (041) and (-104) diffraction planes of catalyst [JCPDS no 71-2274]respectively. X-ray diffraction pattern was calculated using by the Debye-Scherrer formula**[26].** $L=0.89\ \lambda / \beta\ COS\ \theta$ where L is the crystalline size (nm), λ is the wavelength (nm), β is the full width at half maximum intensity (FWHM-in radian), and θ is the Bragg diffraction angle (^{o}) The average crystalline sizes of the Bi_2O_3-TiO_2nanocomposite material products were calculated to be about 25 nm.

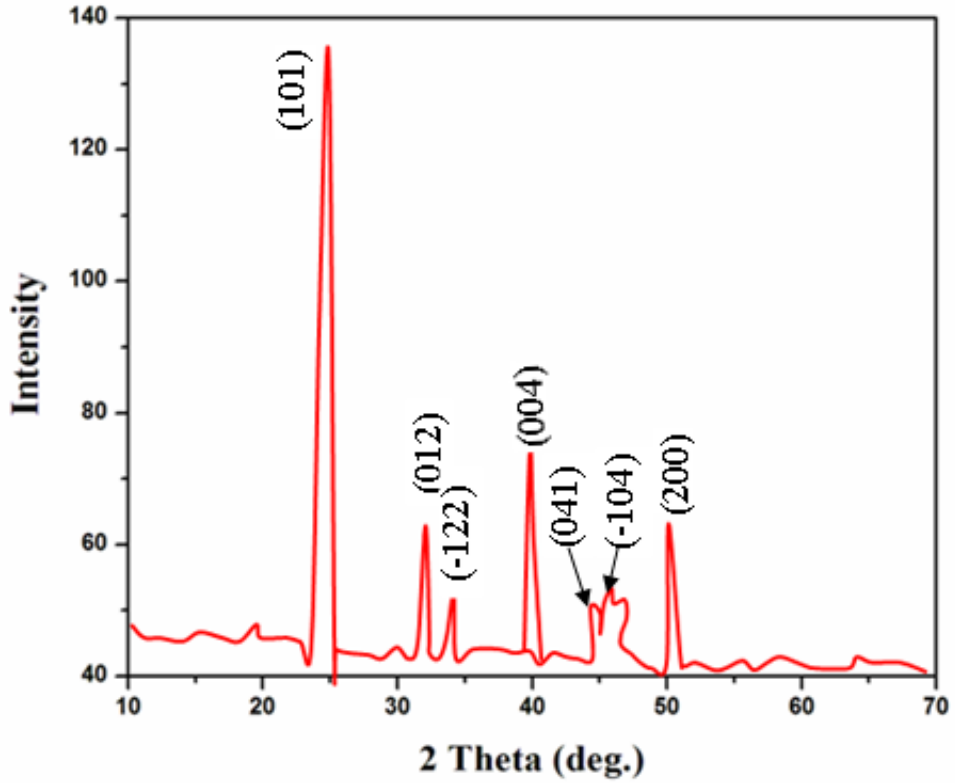

1.6.PL analysis

PL spectra of prepare TiO_2 and Bi_2O_3-TiO_2nanocomposite material as shows in **Fig.4a and b** respectively. As the photoluminescence occurs due to electron-hole recombination, its intensity is directly proportional to the rate of electron –hole recombination its directly proportional to the rate of electron-hole recombination. The prepare TiO_2 it gave two emission at 425 and 480 nm. Prepare $Bi_2O_3$with TiO_2 does not shift the emission of TiO_2but the intensity of PL emission is less when compared to TiO_2 nanocomposite material. This is because of suppression of recombination of electron-hole pairs by which enhance photocatalytic activity

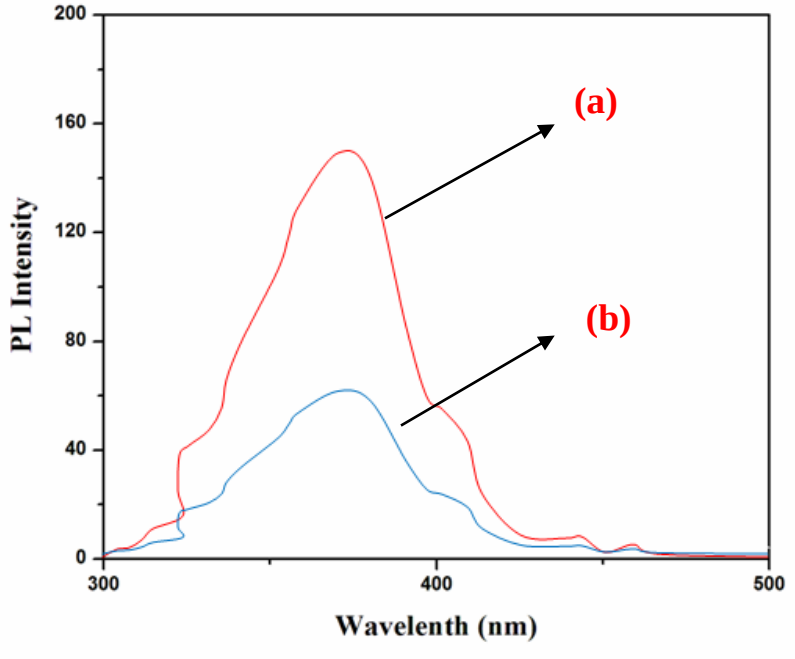

Fig 4. PL analysis (a) TiO_2 and (b) Bi_2O_3-TiO_2 nanocomposite material

1.7.UV-VIS DRS Spectrum

UV-Vis-DRS analysis diffuse reflectance spectra analysis of TiO_2 and Bi_2O_3-TiO_2nanocomposite materialin are displayed in **Fig. 5**. The bio synthesis Bi_2O_3-TiO_2nanocomposite material shows increased absorption in both UV and visible region which is that of TiO_2nanocomposite material can be used as a UV and Visible light active semiconductor photocatalytic nanocomposite material. The UV–Vis spectra is transformed to the Kubelka–Munk function F(R) to separate the extent of light absorption from scattering. The band gap energy is obtained from the plot of the modified Kubelka–Munk function (F(R) E)1/2 versus the energy of the absorbed light E by the Eq. (1)

$$(F(R)\,E)^{1/2} = \frac{\left[(1-R)^{1/2}\right]}{2R} \quad X \quad h\nu \qquad \ldots\ldots\ldots\ldots(1)$$

The final result indicates was band gab energy of the chemical synthesis TiO_2 and Bi_2O_3-TiO_2nanocomposite material which are 3.3 eV and 3.1 eV correspondingly. The lower band gab energy supports for an superior photo catalytic activity.

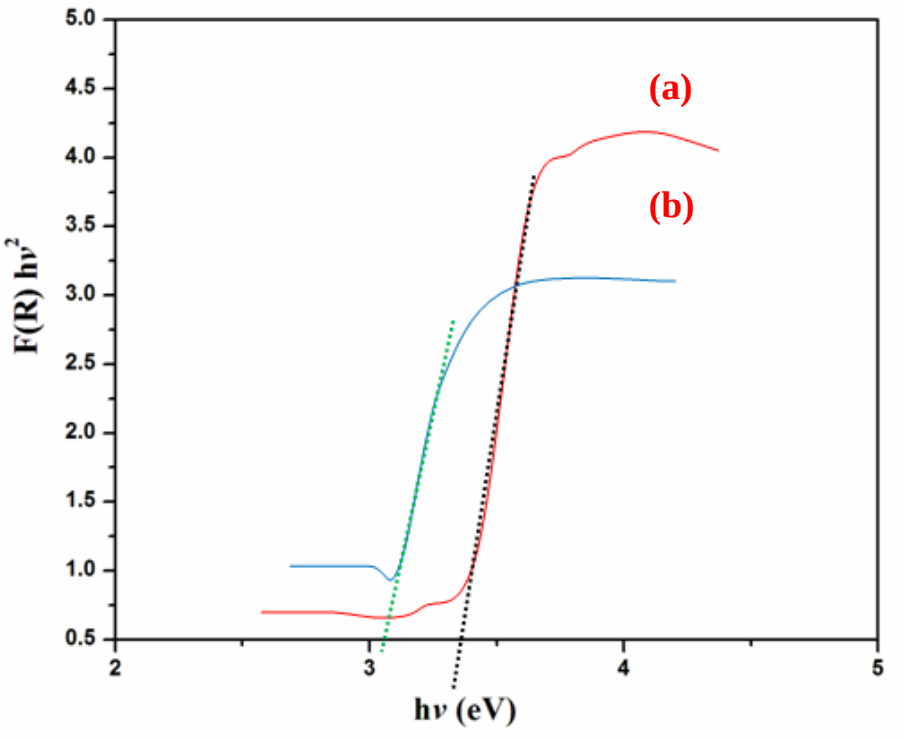

Fig 5. UV-Vis DRS analysis TiO_2 and (b) Bi_2O_3-TiO_2 nanocomposite material

1.8.Catalytic studies

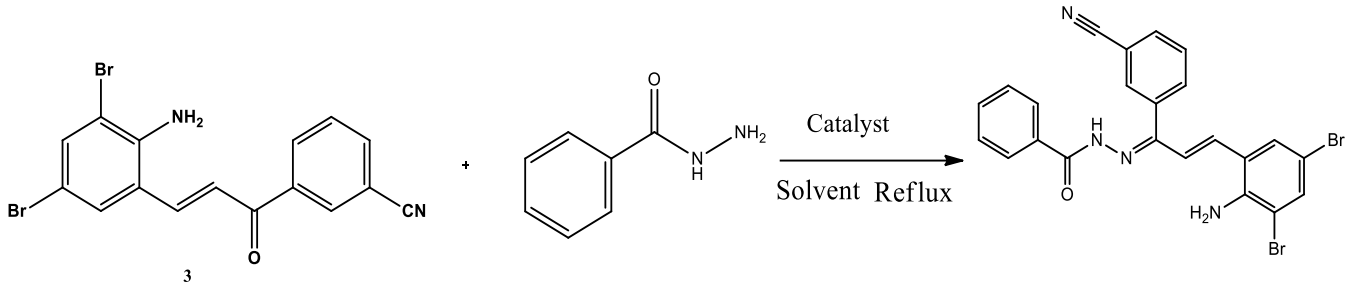

Scheme 1

In order to get effective results, the reaction conditions were optimized. For this purpose, 3-((E)-3-(2-amino-3,5-dibromophenyl)acryloyl)benzonitrile (3), benzohydrazide were used as the model substrate for the synthesis of hydrazone derivatives (4a-e) (Scheme 1). The reaction was monitored by TLC technique using ethyl acetate–hexane (3:7 v/v) as the solvent system. The reaction conditions were optimized in terms of the following reaction variables.

Table 1: Effect of catalyst on reaction time and yield

Initially, a blank reaction was carried out using 3-((E)-3-(2-amino-3,5-dibromophenyl)acryloyl)benzonitrile(3), benzohydrazide for the synthesis of hydrazone derivatives (4a-e). at 100^0 C which resulted in no formation of hydrazone product even after 3 h. The same reaction was carried out using a catalytic amount of Bi_2O_3 - TiO_2 which afforded the desired substituted hydrazone with 92% yield in 60 min

Table 2: Effect of mole percentage of catalyst

Entry	(mol) of Bi_2O_3 - TiO_2	Time (min)	Yield (%)
1	0.1	90	75
2	0.4	60	78
3	0.5	60	92
4	1	60	85

To check the effectiveness of Nano crystalline Bi_2O_3 - TiO_2 with different

Entry	Catalyst	Time (min)	Yield (%)
1	Nano-Bi_2O_3	120	78
2	Nano-TiO_2	120	86
3	Nano-Bi_2O_3 - TiO_2	90	92

catalysts we tried Bi_2O_3, TiO_2, Bi_2O_3 - TiO_2 for the condensation reaction of hydrazone. Bi_2O_3 gave poor yield while TiO_2 gave good yield but required more time as compared to Bi_2O_3 - TiO_2. We observed that Bi_2O_3 - TiO_2 gave good yield with less time compared to other Nano catalyst and the results are shown in Table 1. Thus, it is confirmed from our studies that Bi_2O_3 - TiO_2 was superior for the condensation reaction with good yield in short time.

Table 3: Effect of Solvent on reaction

Entry	Solvent	Temperature (^{0}C)	Time (min)	Yield (%)
1	MeOH	Reflux	90	87
2	EtOH	Reflux	60	92
3	DMF	Reflux	90	78
4	CH_3CN	Reflux	90	69
5	CH_2Cl_2	Reflux	90	72

To optimize the amount of catalyst required for the condensation we tried various mol equivalents of the catalyst compared to the quantity of the hydrazone (Table 2). It was found that when the reaction was carried out with 0.5 mol equivalents reaction was 92%. The condensation reaction was carried out in different solvents such as DMF, MeOH, EtOH, and CH3CN and the results clearly demonstrated that ethanol was found to be the good choice which is shown in Table 3. The yields of the reaction under ethanol solvent conditions were greater and the reaction times were generally shorter than the conventional method.

In order to study the possibility of reusability, the catalyst was filtered, washed with methanol and calcined at 200^0C in an oven for 2 h. The reusability of the catalyst was checked for several successive runs under identical reaction conditions. The catalyst was found to be stable and reusable even after 5 cycles without appreciable loss in activity.

1.9.General proce dure for the preparation of 3-((E)-3-(2-amino-3,5-dibromophenyl)acryloyl)benzonitrile (3):

To a stirred solution of NaOH (50% w/v) in water (5 mL) cooled in an ice bath, a solution of the 3-acetylbenzonitrile and the 2-amino-3,5-dibromobenzaldehyde in ethanol (20 mL) was added drop wise. The reaction mixture was stirred at room temperature overnight. Then the mixture was poured into ice, adjusted to a pH of 3–4 with 1 M HCl, and then filtered. The precipitate was crystallized from ethanol . Yellow crystals. Yield: 85%, m.p.: 125^0C.

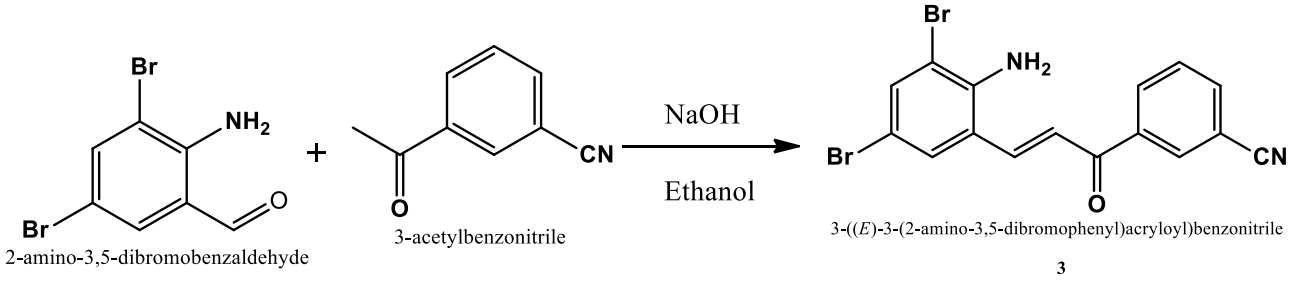

2-amino-3,5-dibromobenzaldehyde

1

3-acetylbenzonitrile

2

3-((*E*)-3-(2-amino-3,5-dibromophenyl)acryloyl)benzonitrile

3

Ethanol

Reflux

BI_2O_3-TiO_2

Compound	Substitution
4a	
4b	
4c	
4d	
4e	

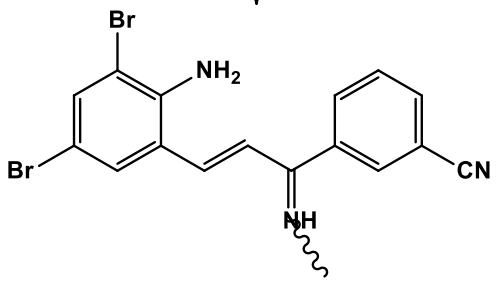

4a-4e

Scheme-2:

The IR spectra of 3-((E)-3-(2-amino-3,5-dibromophenyl)acryloyl)benzonitrile (3) showed a carbonyl absorption at 1655 cm^{-1} which is characteristic band of the α, β- unsaturated carbonyl group. Ethylinic double bond stretching of chalcone showed at 1581 cm^{-1}. C-Br stretching displayed at 536 cm^{-1} A medium to strong absorption band seen at 856 cm^{-1} is due to trans CH=CH out of plane deformation (wagging). The aromatic C-H stretching was observed at 3066 cm^{-1} .

Compound	Color	Mol. Formula	Mol. weight	Solubility	Melting point (°C)
4a	Yellow	$C_{23}H_{16}Br_2N_4O$	524	Ethanol	215
4b	Yellow	$C_{23}H_{15}Br_2ClN_4O$	558	Ethanol	223
4c	Yellow	$C_{24}H_{18}Br_2N_4O_2$	554	Ethanol	286
4d	Yellow	$C_{23}H_{15}Br_3N_4O$	603	Ethanol	245
4e	Yellow	$C_{23}H_{18}Br_2N_4O_2S$	574	Ethanol	312

1.10. General procedure for the preparation of hydrazone derivatives (4a-e):

The hydrazone derivatives of above chalcone were prepared by reacting the respective chalcone (3) and the respective substituted hydrazides in 1:1 stichiometric amounts in minimum amount of ethanol with a 0.5mol nanocatalyst - Bi_2O_3-TiO_2. The reaction mixture was refluxed on the water bath for 60min. Completion of the reaction was monitored by TLC using ethyl acetate–hexane (3:7 v/v) as the developing solvent. Product separated out when the mixture was allowed to cool. It was filtered out, washed with ether and dried in vacuum over anhydrous $CaCl_2$.

Table-4: Physical data of various synthesized compounds

Table 5: Data from IR spectra of Hyrazone derivatives (4a-e)

The IR frequencies of compounds 4a-e is showed in Table 5, in which the C=N stretching frequency appear at 1586-1667 cm^{-1} Aromatic (CH) stretching frequencies appear at 3066-3083cm^{-1} and stretching frequency observed at 1622-1645cm^{-1} C=O group present in the derivatives.

Table 6: Data from ^{1}H NMR spectra of Hyrazone derivatives (4a-e)

Compounds	-NH	NH_2	Aromatic protons
4a	7.2 (1H,singlet)	1.60 (1H,singlet)	7.64-8.59 (13H, multiplet)
4b	7.18 (1H,singlet)	1.52 (1H,singlet)	7.56-8.51 (15H, multiplet)
4c	7.19 (1H,singlet)	1.57 (1H,singlet)	7.59-8.53 (15H, multiplet)
4d	7.18 (1H,singlet)	1.60 (1H,singlet)	7.58-8.51 (15H, multiplet)

Compounds	FREQUENCY cm^{-1}					
	C=O	**C=N**	**C≡N**	**CH=CH**	**N-H**	**ARO C-H**
4a	1622	1586	2230	1470	3459	3066
4b	1645	1586	2230	1469	3436	3067
4c	1645	1589	2231	1412	3437	3070
4d	1625	1586	2231	1470	3465	3067
4e	-	1667	2351	1492	3458	3083
4e	7.19 (1H,singlet)		1.60 (1H,singlet)		7.58-8.50 (15H, multiplet)	

The ^{1}H NMR chemical shift values of compound (**4a-e**) given in **Table.6**. The singlet observed in the range 7.18-7.20ppm is due NH proton. The singlet observed at 1.52-1.60ppm is due $–NH_2$ proton. The signals appearing 7.56-7.89ppm are obviously due to aromatic protons.

Table 7. Data from ^{13}C NMR spectra of Hyrazone derivatives (4a-e)

Compounds	C=N	C=O	Aromatic Carbons	C≡N
4a	155.23	163.16	118.73-143.90	113.31
4b	155.21	163.29	118.70-143.89	113.34
4c	155.31	163.44	118.73-143.92	113.34
4d	155.21	163.24	118.73-143.88	113.31
4e	155.20	-	118.73-143.88	113.31

The ^{13}C chemical shift values of compound (**32**) is given in the **Table 7.**The signal at 113.31-113.34 ppm is assigned to CN carbon. The signal observed at 155.20-155.23ppm is due to (C=N) carbon. The signal observed at 163.16-163.44ppm is due to CO carbon. The chemical shift due to aromatic carbon can be readily sorted out by their characteristic down field absorption in the region 118.70 to 143.92ppm .

1.11. Conclusion

The present work describes a new, efficient and eco-friendly Bi_2O_3-TiO_2 catalyst for the synthesis of substituted hydrazone derivatives (4a-e). The Bi_2O_3-TiO_2 catalyst exhibits excellent catalytic activity for the condensation. Most importantly this catalyst facilitates the reaction at reflux temperature providing solid support in the reaction, enhances the reaction rate and thereby the excellent yields of the products. Therefore, we conclude that the Bi_2O_3-TiO_2 is the best catalyst for the synthesis of substituted hydrazone derivatives (4a-e). The catalyst was also found to be stable and reusable even after 5 cycles without appreciable loss in activity.

Reference

1. Mail kumaran P. et al. Asian Journal of Pharmaceutical Analysis and Medicinal Chemistry. 1(2), 2013, 104 - 109.
2. Szmant, H. H.; McGinnis, C. J. Am. Chem. Soc. 1950, 72, 2890–2892.
3. Hwu, J. R.; Lin, C. C.; Chuang, S. H.; King, K. Y.; Sue, T. R.; Tsay, S. C. Bioorg. Med. Chem. 2004, 12, 2509–2515;
4. Kiasat, A. R.; Kazemi, F.; Nourbakhsh, K. Phosphorus, Sulfur Silicon Relat. Elem. 2004, 179, 569–573.
5. Polshettiwar, V.; Varma, R. S. Tetrahedron Lett. 2007, 48, 5649–5652.
6. Chakraborti, A. K.; Bhagat, S.; Rudrawar, S. Tetrahedron Lett. 2004, 45, 7641–7644.
7. Lalitha, A.; Pitchumani, K.; Srinivasan, C. Green Chem. 1999, 1, 173–174.

8. Niknam, K.; Kiasat, A. R.; Karimi, S. Synth. Commun. 2005, 35, 2231–2236.
9. Yadav, U. N.; Shankarling, G. S. J. Mol. Liq. 2014, 191, 137–141.
10. Parveen, M.; Azaz, S.; Malla, A. M.; Ahmad, F.; da Silva, P. S. P.; Silva, M. R. New J. Chem. 2015, 39, 469–481.
11. Jarikote, D. V.; Deshmukh, R. R.; Rajagopal, R.; Lahoti, R. J.; Daniel, T.; Srinivasan, K. V. Sonochem. 2003, 10, 45–48;
12. Gadhwal, S.; Baruah, M.; Sandhu, J. S. Synlett 1999, 1573–1574.
13. Mokhtari, J.; Naimi-Jamal, M. R.; Hamzeali, H.; Dekamin, M. G.; Kaupp, G. ChemSusChem. 2009, 2, 248–254
14. M. Mazloumi, N. Shahcheraghi, A. Kajbafvala et al., Journal of Alloys and Compounds, vol. 473, no. 1-2, pp. 283–287, 2009.
15. A. Kajbafvala, H. Ghorbani, A. Paravar, J. P. Samberg, E. Kajbafvala, and S. K. Sadrnezhaad, Superlattices and Microstructures, vol. 51, pp. 512–522, 2012.
16. M. R. Bayati, R. Molaei, A. Kajbafvala, S. Zanganeh, H. R. Zargar, and K. Janghorban, Electrochimica Acta, vol. 55, no. 20, pp. 5786–5792, 2010.
17. A. Kajbafvala, J. P. Samberg, H. Ghorbani, E. Kajbafvala, and S. K. Sadrnezhaad, Materials Letters, vol. 67, pp. 342–345, 2012.
18. M. Mazloumi, S. Zanganeh, A. Kajbafvala et al., Ultrasonics Sonochemistry, vol. 16, no. 1, pp. 11–14, 2009.
19. Marimuthu G et al., Egyptian journal of chemistry, doi: 10.21608/ejchem.2019.6248.1524 article in press.
20. A. Kajbafvala, S. Zanganeh, E. Kajbafvala, H. R. Zargar, M. R. Bayati, and S. K. Sadrnezhaad, Journal of Alloys and Compounds, vol. 497, no. 1-2, pp. 325–329, 2010.
21. A. Kajbafvala, M. R. Shayegh, M. Mazloumi et al., Journal of Alloys and Compounds, vol. 469, no. 1-2, pp. 293–297, 2009.
22. A. Lak, M. Mazloumi, M. Mohajerani et al., Journal of the American Ceramic Society, vol. 91, no. 10, pp. 3292–3297, 2008.
23. S. Zanganeh, A. Kajbafvala, N. Zanganeh et al., Applied Physics A, vol. 99, no. 1, pp. 317–321, 2010.
24. M. Mazloumi, M. Attarchi, A. Lak et al., Materials Letters, vol. 62, no. 26, pp. 4184–4186, 2008.
25. S. Zanganeh, M. Torabi, A. Kajbafvala et al., Journal of Alloys and Compounds, vol. 507, no. 2, pp. 494–497, 2010.
26. G. Marimuthu et al., Journal of Biochemical and Technology (2019) 10(2): 28-37
27. Prithivirajan B et al., Biomedical Research 2018; 29 (19): 3590-3598